

Bulk medium evolution has considerable effects on jet observables!

Yasuki Tachibana,¹ Chun Shen,^{1,2} and Abhijit Majumder¹

¹*Department of Physics and Astronomy, Wayne State University, Detroit, MI 48201, USA*

²*RIKEN BNL Research Center, Brookhaven National Laboratory, Upton, NY 11973, USA*

(Dated: January 30, 2020)

We consider the case, in QCD, of a single jet propagating within a strongly interacting fluid, of finite extent. Interactions lead to the appearance of a source of energy-momentum within the fluid. The remnant jet that escapes the container is analyzed along with portions of the medium excited by the jet. We study the effect of a static versus an expanding medium, with jets traveling inward versus outward, considering the medium response via recoils in partonic scatterings based on a weakly-coupled description and its combination with hydrodynamical medium response based on a strongly-coupled description, followed by incorporation into a jet. The effect of these limits on the reconstructed energy, momentum and mass of the jet, as a function of the angle away from the original parton direction are studied. It is demonstrated that different flow velocity configurations in the medium produce considerable differences in jet observables. This work highlights the importance of accurate dynamical modeling of the soft medium as a foundation on which to calculate jet modification, and casts skepticism on results obtained without such modeling.

Over the last several years, the study of jets as probes [1–15] has taken center stage in the exploration of the Quark-Gluon Plasma (QGP), created in nuclear collisions at the Relativistic Heavy-Ion Collider (RHIC) and the Large Hadron Collider (LHC). The first experimental signature of jet quenching was discovered at RHIC through high- p_T hadron suppression [16, 17]. Later, modifications of reconstructed jets were observed at the LHC [18–20]. Developing experimental techniques allow us to investigate jets and jet modification via a variety of observables: Inclusive observables such as the nuclear modification factor [21] and azimuthal anisotropy [22] as well as substructure observables such as the jet fragmentation function [23], jet shape [24], jet mass [25], etc.

Most early calculations of jet quenching used the Bjorken cylinder [26–28] as the background medium: The cross-sectional area was given by the overlap of the two incoming nuclei, while the local entropy density would diminish due to longitudinal expansion, as $s(\tau) = s(\tau_0)\tau_0/\tau$. While such a simplified medium profile was known to yield specious results for some high- p_T hadron observables such as the azimuthal anisotropy v_2 [29, 30], it yielded a fair description of the p_T and centrality dependence of leading hadron suppression [27, 28].

Within the last decade there has been a near sea change in our understanding of jets, from their clustering algorithms [31], the effect of higher orders and resummations [32, 33], to the variety of minor effects that influence their modifications in a dense medium [34–38]. However, in the majority of cases, there has been little improvement in the modeling used to describe the underlying medium that both provides the space-time profile of the energy or entropy density through which the jets propagate, and which the jets can in turn excite.

The argument that, due to asymptotic freedom, a jet will be weakly coupled with the soft medium, and as such an accurate description of the bulk dynamics of the

medium is *not* essential for jet observables, is simply incorrect. Jets include both hard modes (weakly coupled with the medium) and a multitude of soft modes, branched off from the hard modes. These softer modes, that start off as soft partons, interact strongly with the medium constituents, leading to the excitation of the medium. Depending on its energy, a considerable portion of the jet in a heavy-ion collision will consist of softer hadrons that originate from the excited medium.

The medium response has typically been described using weak coupling, strong coupling or some combination between these extremes. A portion of this response is clustered back into the jet and affects its properties. In this Letter, we point out that the bulk dynamics of the underlying medium, by interacting strongly with the softer modes of the jet, exerts an unexpected amount of influence on the properties of the modified jet. In fact, the choice of the bulk medium leads to differences that greatly exceed those caused by the choice of strong or weak coupling as the mechanism of energy-momentum diffusion away from the jet.

To illustrate our point, we use a state-of-the-art event generator as furnished by the JETSCAPE collaboration [39, 40] (JETSCAPE 1.0). The modification of the parton shower in the medium is calculated within a multistage approach, using the MATTER [41, 42] simulator for partons with virtualities $\mu \geq 2$ GeV and the LBT [43, 44] simulator for partons with $\mu \sim 2$ GeV, in the medium. Virtuality refers to the off-shellness of a parton i.e., $\mu^2 = E^2 - p^2 - m^2$. At high virtualities, partons in MATTER undergo a vacuum like virtuality ordered splitting process with later emissions taking place at successively lower virtualities. The scattering in the medium engenders a minor enhancement in the emission rate, by small temporary increments of the virtuality. As virtualities of the later produced partons drop down to a scale comparable to that generated by scatterings in

the medium, one enters the regime of multiple scattering induced emissions. This stage, modeled using the LBT generator, uses the medium modified emission kernel to calculate the rate of the emission, which is induced only by the medium effect. Once the parton escapes the QGP, it may re-enter the MATTER phase without a medium induced portion, if the virtuality is higher than $\mu_{\min} = 1$ GeV.

More details on the partonic portion of this multistage event generator may be found in Ref. [45], and will not be repeated here. The main difference between the calculations in that effort and the current is the value of the jet transport coefficient \hat{q} , which controls the strength of medium induced emissions in both MATTER and LBT. Partons within the jet shower scatter off partons within the medium, this scattering is the source of medium induced radiation. The transport coefficient \hat{q} represents the mean square momentum, transverse to the velocity of the parton, exchanged between it and the medium. We will assume a quasi-particle picture of the medium, as furnished by hard thermal loop effective theory [46, 47]. Given a medium temperature T at the location of the parton i (with energy E_i), one obtains:

$$\hat{q}_i = C_i \alpha_S^{\text{med}} \mu_D T \log \left(\frac{6E_i T}{\mu_D^2} \right). \quad (1)$$

Here, $C_i = C_A$ or C_F is the Casimir color factor for the parton i , α_S^{med} is the in-medium coupling constant, and $\mu_D = gT[(N_c + N_f)/3]^{1/2}$ is the Debye screening mass for a QCD plasma with N_c colors and N_f fermion flavors.

In this Letter, we examine two scenarios for the medium response to jet propagation. One is based on the weakly coupled description in which all processes of energy-momentum exchange between jets and medium are carried out through individual partonic scatterings. The scatterings are simulated as 2-to-2 processes with a jet parton and a parton picked-up from the medium via sampling of the thermal distribution. After the scattering, the outgoing partons, called recoil partons, propagate while interacting with the medium in the same way as jet partons. The energy-momentum deficits (*holes*) left in the medium for the thermal partons sampled in the 2-to-2 interaction are to be subtracted from the final jet energy and momentum. In this scenario, the medium response to jet propagation is constructed by the propagation of recoils and their successive interactions.

The other scenario is the strongly coupled description in which the transport of jet energy and momentum is extended to the hydrodynamic regime. In this scenario, the soft partons with energy below a cut $E_{\text{cut}}^{\text{dep}}$ (as well as the *holes* generated in the 2-to-2 interaction) are assumed to be absorbed in the fluid, and their energy and momentum are diffused until they *thermalize*. Then, the diffused energy and momentum are injected into the medium and evolve hydrodynamically with the bulk medium.

The diffusion process in the strongly coupled description for the medium response is modeled with the causal relativistic diffusion equation [48]:

$$\left[\frac{\partial}{\partial t} + \tau_{\text{relax}} \frac{\partial^2}{\partial t^2} - D_{\text{diff}} \nabla^2 \right] j_i^\nu(x) = 0, \quad (2)$$

with the initial conditions $j_i^\nu = \pm_i p_i^\nu \delta^{(3)}(\vec{x} - \vec{x}_i^{\text{dep}})$ and $\partial j_i^\nu / \partial t = 0$ at $t = t_i^{\text{dep}}$, where \pm_i corresponds to a soft parton being absorbed or a *hole* corresponding to a deficit in the scattering, with an index i , four-momentum p_i^ν , at $(t_i^{\text{dep}}, \vec{x}_i^{\text{dep}})$. Here, D_{diff} is the diffusion coefficient and τ_{relax} is the relaxation time. The speed of signal propagation in Eq. (2) is given by $v_{\text{sig}} = (D_{\text{diff}}/\tau_{\text{relax}})^{1/2}$ and the values of D_{diff} and τ_{relax} are chosen to satisfy $v_{\text{sig}} \leq 1$.

The equation of motion for the fluid with deposited energy and momentum is given by $\partial_\mu T^{\mu\nu}(x) = J^\nu(x)$ [49–51], where $T^{\mu\nu}$ is the energy-momentum tensor of the medium. The source term J^ν can be written as $J^\nu(x) = \sum_i j_i^\nu(x) \delta(t - [t_i^{\text{dep}} + t_{\text{th}}])$, where $j_i^\nu(x)$ is the solution of Eq. (2). We assume the entire energy and momentum source term $j_i^\nu(x)$ thermalizes after a thermalization time t_{th} . The medium is modeled as an ideal fluid with an equation of state (EoS) from Ref. [52].

To investigate how the background medium expansion affects the jet shower evolution and the medium response to it, we employ two different initial profiles of the medium for a systematic comparison. One is a static uniform initial condition, the so-called brick, with infinite size and temperature $T = 0.25$ GeV. The other is given by three-dimensional Gaussian profile of energy density $\epsilon(t = 0, x) = \epsilon_{\text{lat}}(T_0) \exp[-|\vec{x}|^2/(2\sigma^2)]$, where ϵ_{lat} is the energy density at the temperature (T_0) at the center, for the case of an expanding medium fluid. We set $T_0 = 0.5$ GeV and $\sigma = 1.5$ fm. This expanding fluid profile is different from the one used commonly in studies for heavy ion collisions. However, the purpose here is not to give quantitative results directly comparable with experimental data but to carry out systematic studies under controllable configurations. This also allows us to avoid coordinates designed for collider configurations in which the beam axis is taken as a special direction.

In this study, we define the jet energy, momentum, and mass squared as

$$P^\mu(\theta) = \int_0^\theta d\theta' \frac{dP^\mu}{d\theta'}, \quad M^2(\theta) = P^\mu(\theta) P_\mu(\theta), \quad (3)$$

to study how these conserved quantities assigned to the initial parton are recovered by increasing the polar angle θ from the original parton direction. Here, $dP^\mu/d\theta$ is the angular distribution of four-momentum associated with jet propagation, which is obtained with background subtraction appropriate for each type of medium contribution. In the weakly-coupled case, we employ the com-

monly used subtraction method for *hole* partons [43],

$$\frac{dP_{\text{weak}}^{\mu}}{d\theta} = \frac{1}{\Delta\theta} \left[\sum_{\substack{\theta < \theta_i < \theta + \Delta\theta \\ i \in \text{shower} \\ p_i^0 \geq E_{\text{cut}}^{\text{dep}}}} p_i^{\mu} + \sum_{\substack{\theta < \theta_i < \theta + \Delta\theta \\ i \in \text{shower} \\ 0 \leq p_i^0 < E_{\text{cut}}^{\text{dep}}}} p_i^{\mu} - \sum_{\substack{\theta < \theta_j < \theta + \Delta\theta \\ j \in \text{holes}}} p_j^{\mu} \right], \quad (4)$$

where p_i^{μ} and θ_i are parton i 's four-momentum and polar angle from the original parton's direction. In Eq. (4), the sum of the first two terms on the right hand side is taken over all final state partons in the shower. The sum in the last term is taken over all *hole* partons.

On the other hand, in the strongly-coupled description, some portion of jet energy and momentum propagates via hydrodynamic flow in the medium. The fluid part contribution needs to be added to the final jet, i.e.,

$$\frac{dP_{\text{strong}}^{\mu}}{d\theta} = \frac{1}{\Delta\theta} \sum_{\substack{\theta < \theta_i < \theta + \Delta\theta \\ i \in \text{shower} \\ p_i^0 \geq E_{\text{cut}}^{\text{dep}}}} p_i^{\mu} + \left. \frac{dP_{\text{fluid}}^{\mu}}{d\theta} \right|_{\text{w/ jet}} - \left. \frac{dP_{\text{fluid}}^{\mu}}{d\theta} \right|_{\text{w/o jet}}. \quad (5)$$

The result from a hydro simulation without jet propagation is subtracted as the background. Note here that only partons with energy above the cut $E_{\text{cut}}^{\text{dep}}$ exist in the shower in this scenario. To obtain the fluid contribution $dP_{\text{fluid}}^{\mu}/d\theta$, we need to include the effect from medium particlization, which is done via the well known Cooper-Frye prescription [53]:

$$\frac{dP_{\text{fluid}}^{\mu}}{d\theta} = \int dp d\phi |\vec{p}|^2 \sin\theta \left[\sum_i \int_{\Sigma_{\text{FO}}} \frac{p^{\alpha} d^3\sigma_{\alpha}}{p^0} p^{\mu} f_i(x, p) \right], \quad (6)$$

where f_i is the local equilibrium distribution of particles in the medium and the integration in square brackets is over the freeze-out hypersurface Σ_{FO} , for which we use the isochronous surface at $t_{\text{FO}} = 10$ fm/c for simplicity.

To see the hydrodynamic transport directly i.e., without particlization, we calculate the medium contribution from the energy-momentum tensor of the fluid:

$$\frac{dP_{\text{fluid}}^{\mu}}{d\theta} = \int d^3x T^{0\mu}(t_{\text{FO}}, \vec{x}) \delta(\theta - \theta_T), \quad (7)$$

where θ_T is the polar angle of fluid momentum T^{0i} with respect to the jet direction. For the subtracted background in the brick case, we take the limit of $T^{0i} \rightarrow 0$ for all spatial components.

In this work, we perform simulations of jet evolution in vacuum, a static brick, and an expanding medium, starting with a single gluon of energy $p_{\text{init}}^0 = 140$ GeV. Its momentum amplitude is determined by sampling the Sudakov form factor in MATTER, with a direction along the x -axis. The jet partons evolve up to $t = 8$ fm. For vacuum simulations, we apply MATTER without medium effects. In-medium energy loss is modelled by MATTER and LBT with $\alpha_S^{\text{med}} = 0.25$, above $T = 160$ MeV.

In the weakly-coupled case, the medium evolves according to the hydrodynamic equation without a source

term. In the strongly-coupled description, we introduce source terms generated by the relativistic diffusion equation (2) for the *hole* partons and soft partons with the energy in the lab frame below the cut $E_{\text{cut}}^{\text{dep}} = 2$ GeV. We set $\tau_{\text{relax}} = 1.0$ fm, $D_{\text{diff}} = 0.6$ fm, and $t_{\text{th}} = 1.5$ fm.

Figure 1 shows the angular distribution of the jet observables defined in Eq. (3). For the case with the expanding medium, we consider two different production points of the jet initiating parton; the parton is produced at the center of the medium ($x = y = z = 0$) and escapes *outward* along with the radial flow, or the parton is produced at the edge ($x = -10$ fm, $y = z = 0$) and propagates *inward*, toward the center against the radial flow.

It should be noted that all jet energies, momenta, and masses squared, for all settings, converge to their original values, which are assigned to the jet initiating parton, at $\theta = \pi$, showing their conservation during the evolution. This also serves as a crucial test of our calculation. The jet substructures are modified within the constraints of these conservation conditions.

In the case of the brick: The results from the strongly coupled scenario without particlization (dashed-blue lines) indicate that the energy momentum propagation is spread away from the initial jet direction, appearing in directions both behind and away from the jet, with the energy recovered monotonically. Meanwhile, the momentum increases sharply until $\theta = \pi/2$ and then very slowly decreases to its full value at π . Remarkably, this structure with momentum larger than energy gives a negative value of the mass squared over a wide range of θ .

Particlization causes a suppression of energy-momentum emission in the direction opposite to the jet. It drastically modifies the jet structure by flipping the order of how the net energy and momentum approach to their full values around $\theta = \pi$. This is a consequence of the subtraction of the locally boosted equilibrium distribution used in Eq. (6). The particle distribution in a fluid element with flow velocity, which tends to be in the jet direction caused by jet-energy deposition, gives less particles with momentum opposite to the flow, but more particles in the flow direction, than the isotropic distribution in a static fluid.

The results from the weakly coupled scenario show qualitatively the same trends as in the strong particlized case (dotted-green lines vs. solid-red lines). In a static medium, the subtraction prescription for *hole* partons, in Eq. (4), can somewhat mimic the backward suppression as well as the broadening. Some medium partons involved in the scatterings can initially have momentum opposite to the jet direction and be bounced forward.

In the case of jet propagation outward: From the expanding medium, the strong radial flow following the jet pushes the transported energy and momentum forward. This blue-shift generates a focus effect and makes the broadening of the energy and momentum response distribution more moderate than the static situation. In

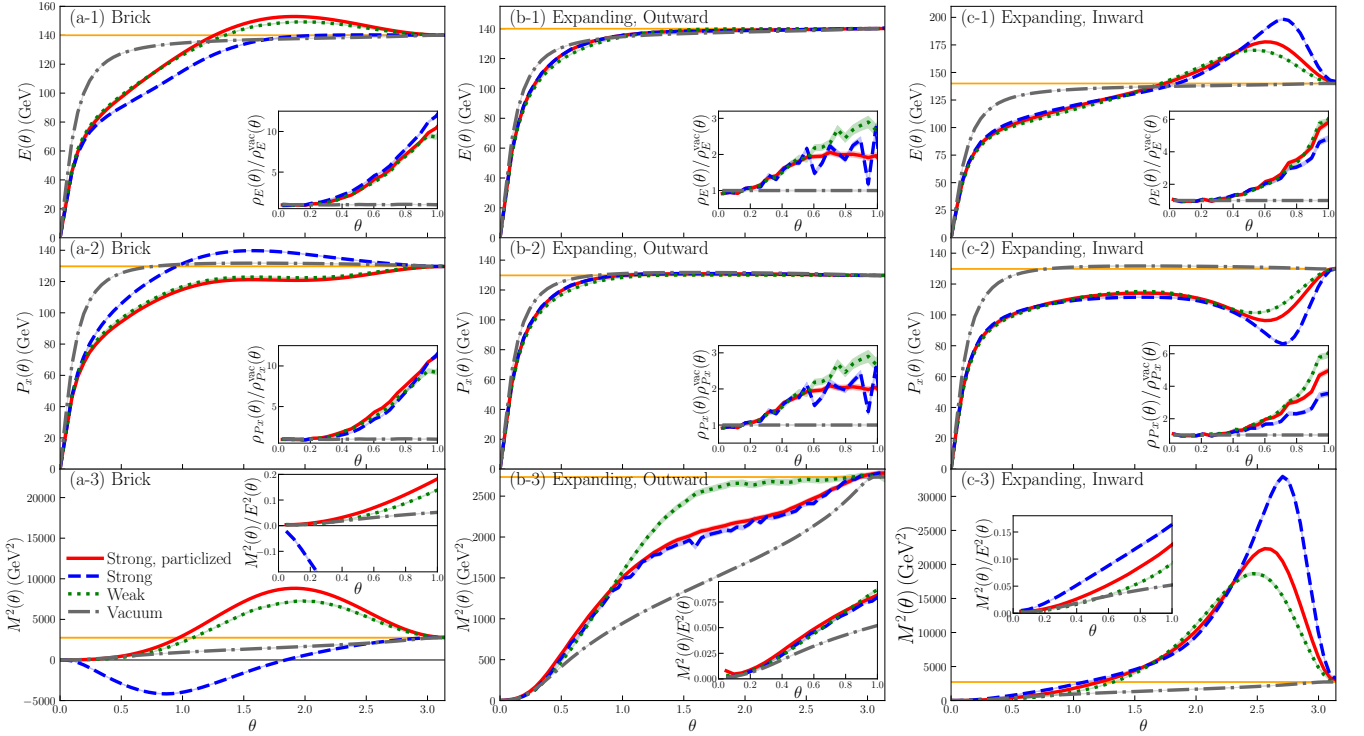


FIG. 1. (Color online) Jet energy, momentum in the direction of the initial parton, and mass squared as a function of the opening angle θ for the jets propagating in the brick medium (a-1)-(a-3), outward along the expanding medium (b-1)-(b-3), and inward against the expanding medium (c-1)-(c-3). The solid-red lines and dashed-blue lines are the results including the hydrodynamic response effect in a strongly-coupled description with and without particlization, respectively. The dotted-green lines show the results with the medium response within a weakly-coupled description by recoils. The dot-dashed grey lines represent vacuum simulations. The horizontal solid orange lines indicate the average values assigned to the initial parton.

this case, the particlization effect is very negligible. This is because most particles in a fluid element with a very large flow velocity tend to be aligned with the flow velocity. Thus, the fluid elements can not emanate particles opposed to the strong radial flow of the medium, regardless of the direction of the jet-induced flow. Therefore, the backward over subtraction does not happen. In the expanding medium case, the angular evolution of jet mass shows a clear difference between the weakly- and strongly-coupled scenarios when $\theta > 1$. This is because the medium partons excited in the weakly-coupled scenario are sampled from the local temperature and flow velocity at jet splitting. This particle distribution is different from those particlized from fluid cells at the switching surface for the particlization.

In the case of jet propagation inward: In this case, the jet-induced flow following the jet dams up and deflects off the opposing radial flow in the strongly coupled scenario. Thereby, the momentum radiated from the jet is pushed in the backward direction. These deflected vectors continue to add to the energy accumulated in the backward direction. These structures after the particlization are smeared but still shows the same tendency. In the weakly coupled scenario, the recoil partons with multiple successive collisions can somewhat mimic the jet-induced flow, as they are sampled from the oppositely flowing medium.

To see detailed structure around the jet direction, we also show the jet energy and momentum shapes,

$$\rho_E(\theta) = \frac{1}{E(\theta=0.4)} \frac{dE}{d\theta}, \quad \rho_{P_x}(\theta) = \frac{1}{P_x(\theta=0.4)} \frac{dP_x}{d\theta}, \quad (8)$$

scaled by their vacuum results, and mass squared scaled by energy squared $[M^2(\theta)/E^2(\theta)]$, for the range of $0 \leq \theta \leq 1$ in the insets of Fig. 1. One can see that the medium flow effects which cause the unique structures at large angles $\theta \gtrsim \pi/2$ also affect the jet inner-structure. In particular, the difference between the various scenarios for the dynamics of the bulk medium appears clearly in the response of the medium to the jet: The strongly-coupled description gives a weaker energy and momentum broadening, compared to the weakly-coupled case, for both following and opposing flows, and larger jet mass for opposing flow with opening angle $\theta < 1$.

In summary, we have systematically studied jet structure modification in a static or an expanding fluid with medium response effects. It is shown that the flow velocity of the background medium predominantly affects the in-medium transport of jet quantities, such as energy, momentum and mass. The medium flow pattern causes further differences in the jet structure with different modeling approaches of medium response. This work demonstrates the indispensable importance for the

realistic modeling of QGP dynamics to study the precise modification of jets in heavy-ion collisions. Such a precision framework can further shed light on studies applying jets as sources of acoustic probes for the flowing medium.

Acknowledgements. The authors are grateful to S. Cao for useful discussions. This work was supported in part by the National Science Foundation (NSF) within the framework of the JETSCAPE collaboration under grant number ACI-1550300, by the U.S. Department of Energy (DOE) under grant number DE-SC0013460.

-
- [1] J. D. Bjorken, Fermilab, Report No. FERMI-LAB-PUB-82-059-THY (unpublished).
- [2] R. Baier, Y. L. Dokshitzer, A. H. Mueller, S. Peigne, and D. Schiff, *Nucl. Phys.* **B483**, 291 (1997), [hep-ph/9607355](#).
- [3] R. Baier, Y. L. Dokshitzer, A. H. Mueller, S. Peigne, and D. Schiff, *Nucl. Phys.* **B484**, 265 (1997), [hep-ph/9608322](#).
- [4] B. G. Zakharov, *JETP Lett.* **63**, 952 (1996), [arXiv:hep-ph/9607440](#).
- [5] M. Gyulassy, P. Levai, and I. Vitev, *Nucl. Phys.* **B571**, 197 (2000), [arXiv:hep-ph/9907461](#).
- [6] M. Gyulassy, P. Levai, and I. Vitev, *Phys. Rev. Lett.* **85**, 5535 (2000), [nucl-th/0005032](#).
- [7] M. Gyulassy, P. Levai, and I. Vitev, *Nucl. Phys.* **B594**, 371 (2001), [arXiv:nucl-th/0006010](#).
- [8] U. A. Wiedemann, *Nucl. Phys.* **B588**, 303 (2000), [arXiv:hep-ph/0005129](#).
- [9] U. A. Wiedemann, *Nucl. Phys.* **A690**, 731 (2001), [arXiv:hep-ph/0008241](#).
- [10] X.-F. Guo and X.-N. Wang, *Phys. Rev. Lett.* **85**, 3591 (2000), [arXiv:hep-ph/0005044](#).
- [11] X.-N. Wang and X.-F. Guo, *Nucl. Phys.* **A696**, 788 (2001), [arXiv:hep-ph/0102230](#).
- [12] A. Majumder, *Phys. Rev.* **D85**, 014023 (2012).
- [13] P. Arnold, G. D. Moore, and L. G. Yaffe, *JHEP* **11**, 057 (2001), [hep-ph/0109064](#).
- [14] P. Arnold, G. D. Moore, and L. G. Yaffe, *JHEP* **06**, 030 (2002), [hep-ph/0204343](#).
- [15] A. Majumder and M. Van Leeuwen, *Prog. Part. Nucl. Phys.* **66**, 41 (2011), [arXiv:1002.2206 \[hep-ph\]](#).
- [16] K. Adcox *et al.* (PHENIX), *Phys. Rev. Lett.* **88**, 022301 (2002), [nucl-ex/0109003](#).
- [17] J. Adams *et al.* (STAR), *Phys. Rev. Lett.* **91**, 172302 (2003), [arXiv:nucl-ex/0305015 \[nucl-ex\]](#).
- [18] G. Aad *et al.* (ATLAS), *Phys. Rev. Lett.* **105**, 252303 (2010), [arXiv:1011.6182 \[hep-ex\]](#).
- [19] S. Chatrchyan *et al.* (CMS), *Phys. Rev.* **C84**, 024906 (2011), [arXiv:1102.1957 \[nucl-ex\]](#).
- [20] B. Abelev *et al.* (ALICE), *JHEP* **03**, 013 (2014), [arXiv:1311.0633 \[nucl-ex\]](#).
- [21] G. Aad *et al.* (ATLAS), *Phys. Rev. Lett.* **114**, 072302 (2015), [arXiv:1411.2357 \[hep-ex\]](#).
- [22] G. Aad *et al.* (ATLAS), *Phys. Rev. Lett.* **111**, 152301 (2013), [arXiv:1306.6469 \[hep-ex\]](#).
- [23] G. Aad *et al.* (ATLAS), *Phys. Lett.* **B739**, 320 (2014), [arXiv:1406.2979 \[hep-ex\]](#).
- [24] S. Chatrchyan *et al.* (CMS), *Phys. Lett.* **B730**, 243 (2014), [arXiv:1310.0878 \[nucl-ex\]](#).
- [25] S. Acharya *et al.* (ALICE), *Phys. Lett.* **B776**, 249 (2018), [arXiv:1702.00804 \[nucl-ex\]](#).
- [26] M. Gyulassy, I. Vitev, X.-N. Wang, and P. Huovinen, *Phys. Lett.* **B526**, 301 (2002), [arXiv:nucl-th/0109063](#).
- [27] I. Vitev and M. Gyulassy, *Phys. Rev. Lett.* **89**, 252301 (2002), [arXiv:hep-ph/0209161 \[hep-ph\]](#).
- [28] C. A. Salgado and U. A. Wiedemann, *Phys. Rev.* **D68**, 014008 (2003), [arXiv:hep-ph/0302184 \[hep-ph\]](#).
- [29] A. Majumder, *Phys. Rev.* **C75**, 021901 (2007), [arXiv:nucl-th/0608043](#).
- [30] S. A. Bass, C. Gale, A. Majumder, C. Nonaka, G.-Y. Qin, *et al.*, *Phys. Rev.* **C79**, 024901 (2009), [arXiv:0808.0908 \[nucl-th\]](#).
- [31] M. Cacciari, G. P. Salam, and G. Soyez, *JHEP* **04**, 063 (2008), [arXiv:0802.1189 \[hep-ph\]](#).
- [32] M. Dasgupta, F. Dreyer, G. P. Salam, and G. Soyez, *JHEP* **04**, 039 (2015), [arXiv:1411.5182 \[hep-ph\]](#).
- [33] Z.-B. Kang, F. Ringer, and I. Vitev, *JHEP* **10**, 125 (2016), [arXiv:1606.06732 \[hep-ph\]](#).
- [34] M. H. Thoma and M. Gyulassy, *Nucl. Phys.* **B351**, 491 (1991).
- [35] A. Majumder, *Phys. Rev.* **C80**, 031902 (2009), [arXiv:0810.4967 \[nucl-th\]](#).
- [36] A. Beraudo, J. G. Milhano, and U. A. Wiedemann, *Phys. Rev.* **C85**, 031901 (2012), [arXiv:1109.5025 \[hep-ph\]](#).
- [37] N. Borghini and U. A. Wiedemann, (2005), [arXiv:hep-ph/0506218 \[hep-ph\]](#).
- [38] A. Majumder, C. Nonaka, and S. A. Bass, *Phys. Rev.* **C76**, 041902 (2007), [arXiv:nucl-th/0703019](#).
- [39] J. H. Putschke *et al.*, (2019), [arXiv:1903.07706 \[nucl-th\]](#).
- [40] A. Kumar *et al.* (JETSCAPE), (2019), [arXiv:1910.05481 \[nucl-th\]](#).
- [41] A. Majumder, *Phys. Rev.* **C88**, 014909 (2013), [arXiv:1301.5323 \[nucl-th\]](#).
- [42] S. Cao and A. Majumder, (2017), [arXiv:1712.10055 \[nucl-th\]](#).
- [43] T. Luo, S. Cao, Y. He, and X.-N. Wang, *Phys. Lett.* **B782**, 707 (2018), [arXiv:1803.06785 \[hep-ph\]](#).
- [44] Y. He, S. Cao, W. Chen, T. Luo, L.-G. Pang, and X.-N. Wang, *Phys. Rev.* **C99**, 054911 (2019), [arXiv:1809.02525 \[nucl-th\]](#).
- [45] S. Cao *et al.* (JETSCAPE), *Phys. Rev.* **C96**, 024909 (2017), [arXiv:1705.00050 \[nucl-th\]](#).
- [46] X.-N. Wang, *Phys. Lett.* **B485**, 157 (2000), [arXiv:nucl-th/0003033 \[nucl-th\]](#).
- [47] S. Caron-Huot and C. Gale, *Phys. Rev.* **C82**, 064902 (2010), [arXiv:1006.2379 \[hep-ph\]](#).
- [48] M. A. Aziz and S. Gavin, *Phys. Rev.* **C70**, 034905 (2004), [arXiv:nucl-th/0404058 \[nucl-th\]](#).
- [49] Y. Tachibana, N.-B. Chang, and G.-Y. Qin, *Phys. Rev.* **C95**, 044909 (2017), [arXiv:1701.07951 \[nucl-th\]](#).
- [50] W. Chen, S. Cao, T. Luo, L.-G. Pang, and X.-N. Wang, *Phys. Lett.* **B777**, 86 (2018), [arXiv:1704.03648 \[nucl-th\]](#).
- [51] N.-B. Chang, Y. Tachibana, and G.-Y. Qin, *Phys. Lett.* **B801**, 135181 (2020), [arXiv:1906.09562 \[nucl-th\]](#).
- [52] S. Borsanyi, Z. Fodor, C. Hoelbling, S. D. Katz, S. Krieg, and K. K. Szabo, *Phys. Lett.* **B730**, 99 (2014), [arXiv:1309.5258 \[hep-lat\]](#).
- [53] F. Cooper and G. Frye, *Phys. Rev.* **D10**, 186 (1974).